Cosmic Dust Collection in Aerogel

Mark J. Burchell,[1] Giles Graham,[2] and Anton Kearsley[3]

[1]Centre for Astrophysics and Planetary Science, School of Physical Sciences, University of Kent, Canterbury CT2 7NR, United Kingdom; email: m.j.burchell@kent.ac.uk

[2]Institute of Geophysics and Planetary Physics, Lawrence Livermore National Laboratory, Livermore, California, 94551; email: graham42@llnl.gov

[3]Department of Mineralogy, Natural History Museum, London SW7 2AZ, United Kingdom; email: antk@nhm.ac.uk

Annu. Rev. Earth Planet. Sci. 2006. 34:385–418

First published online as a Review in Advance on January 16, 2006

The *Annual Review of Earth and Planetary Science* is online at earth.annualreviews.org

doi: 10.1146/annurev.earth.34.031405.124939

0084-6597/06/0530-0385$20.00

Key words

hypervelocity, impact, comet, asteroid

Abstract

Aerogel is an ultra-low-density material that can be used to capture small particles incident upon it at speeds in excess of 1 km s^{-1}. This permits capture of cosmic dust in space where the high speeds usually result in destructive impact events. The performance of aerogel in laboratory impact tests is described. Completely intact capture is rare; most studies show that between 10% to 100% of the incident particle's mass is captured. However, in all cases unaltered domains were found in the particles captured in the laboratory at speeds up to 6 or 7 km s^{-1}. Several analytic techniques can be applied in situ to particles captured in aerogel, yielding data on the preimpact composition of the particle. Extraction techniques for removing small particles from aerogel are described, and after extraction, handling and analysis in the laboratory can proceed as for any small-sized particle. Coupled with the survival of intact regions in the captured particles, this allows detailed identification of the composition of the dust. Examples are given of current space missions using aerogel dust collectors: Data on these will soon be supplemented by cometary dust particles captured in aerogel on the NASA *Stardust* spacecraft.

INTRODUCTION

A key motto often heard in relation to the Solar System is "large is rare." By implication, small is frequent. Dust particles pervade the Solar System. There are many sources of dust, the most obvious are perhaps comets, but asteroids and other atmosphere-less bodies will release dust after impacts and collisions. Volcanic activity on natural satellites can eject dust into space (e.g., Io; see Grün et al. 1993, Graps et al. 2000) and planetary magnetic fields can accelerate the dust (if charged) to high speeds and eject it into interplanetary space at speeds that can exceed the Solar System escape velocity. Interstellar space is filled with dust that can penetrate even into the inner heliosphere (Grün et al. 1993).

The scientific study of cosmic dust has a history of its own and continues today (e.g., Brownlee 1985, Grün et al. 2001). There are several techniques available for dust detection and measurement in environments distant to anthropogenic contamination. A simple one is collection of dust from the stratosphere (Bradley et al. 1983), but this is subject to bias owing to modification in the atmosphere before capture. Measurements in space are therefore desirable. One widely used method is impact ionization, where the impact of dust (submicron- to micron-sized) at high speed on a metal surface vaporizes the impactor and part of the target, generating a plasma whose properties can be measured electronically (see Auer 2001 for a review). Such detectors are relatively simple and robust and can return data concerning impact speed and particle mass and flux. If the detector entrance is collimated and the pointing history is controllable/known, trajectory information can also be obtained. Indeed, if operated in a time of flight collection mode, data can also be provided on elemental composition of the particle (e.g., see Kempf et al. 2005). Such electronic devices can be deployed wherever a spacecraft can be sent and provide a real-time electronic stream of data.

However, other approaches are possible. If a spacecraft (or part thereof) is retrieved at the end of its mission, then passive detectors can be deployed, or exposed surfaces examined, with a view to dust measurements. Apart from short-duration missions, such as sounding rockets, etc., it was the start of the era of the space shuttle and of regularly visited space stations that really permitted use of long-duration passive instruments. An early such device for dust studies was the capture cell (e.g., McDonnell et al. 1984). Such a cell is basically a thin layer of material covering an empty space, the back of which is a thick metal surface. Holes in the entrance layer indicate the location of impacting dust particles, and the rear surface preserves the impact crater (or spray if the particle was disrupted by its passage through the foil), which can then be studied to give the elemental content of the original particle.

However, if a suitable highly porous material could be obtained, the cavity in the capture cell can be filled in. An incident dust particle would then be slowed to rest in the porous capture medium and subsequently in the laboratory a relatively intact dust particle extracted for analysis. This is potentially a far superior situation to analysis of residues and impact debris. During the 1980s, various low-density media were considered as capture media. Foams were considered promising (Tsou et al. 1989, 1991; Tsou 1990; Ishibashi et al. 1990) along with silica tiles (Werle et al. 1981). However, locating the captured particles in such materials proved difficult. What is

required is a low-density, highly porous, transparent medium. The solution chosen was from a family of materials known as aerogels. The one chosen is a dried silica gel (SiO_2) whose final density is controlled during manufacture, with densities of less than 4 kg m^{-3} being achievable. The low-density medium permits a relatively gradual slowing of the incident particle during impact. The transparent nature of silica aerogel allows relatively easy location and observation of the captured particle. Since the first laboratory demonstration that aerogel can capture high-speed particles relatively intact (Tsou et al. 1988), aerogel capture cells have been deployed in low Earth orbit (LEO) on a number of occasions. A current space mission (the NASA *Stardust* mission; Brownlee et al. 2003) has carried aerogel away from the Earth into interplanetary space to capture dust freshly ejected from a comet nucleus and return it to Earth for laboratory analysis.

LEO: low Earth orbit

In this review, the nature of aerogel, its capture properties as determined in the laboratory, its deployment in space, and the range of suitable analysis techniques for the captured particles are described.

AEROGEL MANUFACTURE AND COMPOSITION

Aerogel was developed in the 1930s (Kistler 1931) and is usually a dried silica gel, consisting of long intertwined chains of small spheres of amorphous silica. A rigid three-dimensional structure is obtained with an open system of pores, which gives the low density of the material. The density of the aerogel can be selected during manufacture. In addition, if care is taken during the manufacture process, good optical transparency can also be obtained.

There are several methods of producing silica aerogels. In the single-step process, the initial sol-gel is made, for example, by adding water to tetraalkoxysilane [or tetramethoxysilane (TMOS)] in the presence of a catalyst (e.g., NH_4OH) to produce hydrolysis and condensation of the silicon alkoxides. The final density is controlled by varying the amount of solvent added at this stage. The gel is then left to age for several days. This allows the bonds between the colloidal particles in the gel to strengthen. The initial aging is in a soak solution covering the gel, this is then removed and the sample covered in ethanol (or methanol for TMOS) to help drive out the excess water from the gel. At this stage, the material is known as an alcogel. The aged alcogel is then heated under pressure in an autoclave for supercritical extraction of the solvent (here ethanol or methanol). This typically involves raising the pressure to 125 to 150 bar and the temperature to 225°C to 300°C over a period of 24 to 36 h, during which venting of the alcohol starts. After the temperature and pressure have been raised appropriately (**Figure 1**), the pressure is released while the temperature is maintained, permitting extraction of the remaining alcohol vapor. The aerogel that emerges from the autoclave may still not be totally clear of alcohol, particularly at the surface, so a final bake out in air at a temperature of several hundred degrees Celsius is often the final step in manufacture. The supercritical solvent extraction as described produces a hydrophobic aerogel, but if this step is done via carbon dioxide supercritical techniques at lower temperatures a hydrophilic aerogel results. Similar schemes to that given here are described in detail in Poelz & Reithmuller (1982) and Adachi et al. (1995).

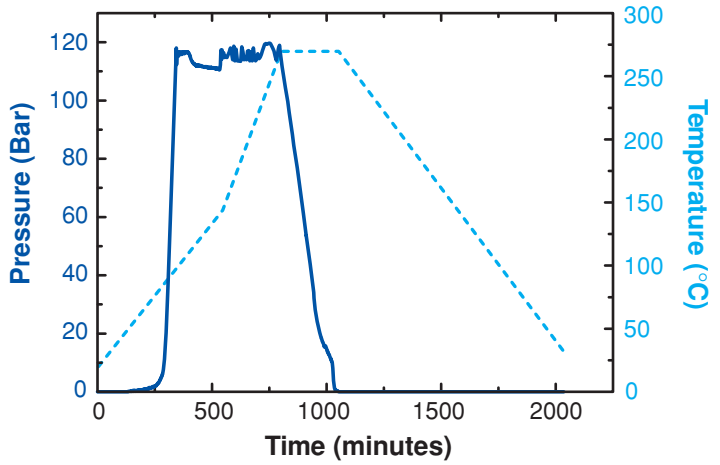

Figure 1

Pressure (*dark blue solid line*, *left axis*) and temperature (*light blue dashed line*, *right axis*) versus time for aerogel manufacture.

A second method of manufacture is also possible, a so-called two-step process (Hrubesh & Poco 1990, Tillotson & Hrubesh 1992, Hrubesh 1998). This is particularly suitable for ultralow aerogel densities below 10 kg m^{-3} (Tsou 1995). Here the first step involves partial hydrolysis and condensation. Water is then added to complete the hydrolysis and produce the gel. The alcogel is then converted to an aerogel by supercritical extraction of the solvent as before.

For particle capture in space, the aerogel purity is an issue of concern, as there is a desire to avoid the aerogel contaminating any subsequent compositional analysis of the captured particle. This issue has been addressed since soon after aerogel was identified as a suitable capture medium. Using a laser microprobe and mass spectrometer, Hartmetz et al. (1990a) analyzed aerogel samples for trace contaminants. They found trace contamination from the TMOS compounds and solvents used in manufacturing their aerogel and that this varied with aerogel density. They observed every atomic mass/atomic number (m/z) value from 10 to 180. They reported that baking the aerogel to 250°C reduced this contamination, but that even so, the aerogel still had the potential to add trace signals to any subsequent compositional analysis. This would make a volatile element analysis of captured dust particles difficult. Further, if any aerogel adhered to the captured particle after extraction, contamination from the aerogel would impede a definitive volatile analysis (Hartmetz et al. 1990b). To reduce this, an even higher temperature bakeout of the aerogel before use (up to 500°C) was recommended, combined with efforts to reduce the volatile content during manufacture.

The carbon content of aerogels (particularly important for analysis of organic content of captured particles) was investigated (Gibson et al. 1991), and it was found that aerogels (density 20–120 kg m^{-3}) had carbon contents ranging from 0.18% to 3.5%, with the greatest content at the lowest densities. Barrett et al. (1992) looked at the water and volatile content of aerogels. They found that the content varied from 0.9% to 8.0% by weight, although no clear association with aerogel density was found. Heating at temperatures up to 150°C removed the water content (typically 1% or

2% by weight), but the majority of the organic contaminants were only removed by a bakeout at 350°C to 600°C (or under vacuum conditions, at lower temperatures, e.g., 250°C). The carbon content of aerogel can be reduced by the use of supercritical fluids, such as carbon dioxide, as ultraclean solvents (Huang et al. 1993). This produced carbon contents of 0.18% to 0.27% by weight. Bakeouts at 600°C removed up to 85% of this contamination; however, such temperatures can also damage the structure of the aerogel, effectively collapsing some of the pore structure, significantly increasing the density of the material, and making it ineffective as a capture medium. This latter problem can be avoided by a stepped heating of the aerogel (Wright et al. 1994).

The Stardust aerogels were examined in detail both for inorganic and organic trace content (Tsou et al. 2003). Many elements were present at less than a few parts per billion, but some, such as aluminum, boron, calcium, germanium, iron, magnesium, sodium, and zinc, were present at the level of a few thousand parts per billion, and tin was present at the level of a few tens of thousand parts per billion. The organic content was found to be on the order of a few percent of the total aerogel mass. This was reduced by baking at 300°C for 72 h (higher temperatures caused shrinkage of the aerogels), which reduced the carbon content of the flight aerogels to <0.5%. However, postflight tests will be required on the flight aerogel to see if this has changed during the time (more than 7 years) since integration and launch. On this latter point, as well as a need for purity control during manufacture and storage, Nishioka et al. (1996) point out that the method used to bond the aerogel into its holder for deployment on a space mission can also introduce contamination and thus needs consideration.

The need for manufacture of aerogel with low volatile content, combined with prolonged vacuum bakeouts and subsequent storage of the aerogel in a clean environment prior to use, has thus been clearly established. If during capture, molten aerogel adheres to the particle, this material can possibly bias subsequent trace volatile analysis. Potentially, this can also be effected by the release (and possible reabsorption) of volatiles from the aerogel by the heating that occurs during capture.

LABORATORY DEMONSTRATIONS OF CAPTURE

The classic particle capture in aerogel at high speed produces a carrot-shaped track near the end of which is found a relatively intact particle (**Figures 2** and **3**). The track can easily be seen in the transparent aerogel. It has an entrance hole (**Figure 4**) that is larger than the cross-sectional area of the particle. Beyond the entrance, the track quickly widens by approximately 50% and then slowly tapers along its length until it is the particle size. The track is typically in line with the impact direction until near its end, where the particle may deviate significantly from this direction. The captured particle may have acquired a partial wrap of molten aerogel during its capture.

When considering the use of aerogel as a capture medium for particles in space, the impact speed is important. In LEO, the typical impact speed of man-made debris is in the range of 7 to 11 km s^{-1} and is typically 20 to 25 km s^{-1} for dust from interplanetary space. Indeed, if the dust is interstellar or from a prograde long-period comet, it can be as high as 60 to 70 km s^{-1}. Specific impact speeds may be determined

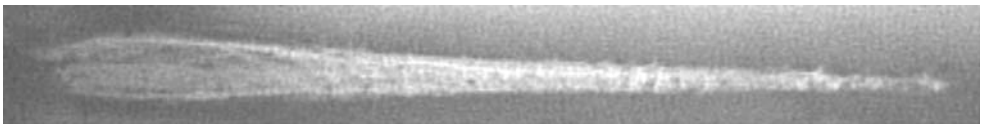

Figure 2

Classic track in aerogel of a captured particle. Impact was from left to right.

for particular space missions. For example, the NASA Stardust mission has used aerogel to capture cometary dust at 6.1 km s^{-1} (see below). Unfortunately, not all these speeds are achievable in laboratory experiments at the required particle sizes. The two main techniques for particle acceleration are (*a*) the two-stage light gas gun and (*b*) the Van de Graaff accelerator. The former can only achieve speeds of 8 to 10 km s^{-1} at most, but can do so for millimeter-sized particles. The latter can achieve speeds of up to 100 km s^{-1} but only for submicron-sized dust grains. Indeed, in a Van de Graaff dust accelerator, particle size and speed are inversely correlated (e.g., see Burchell et al. 1999a); a 1 micron particle is typically accelerated to 3 to 5 km s^{-1}, and it is the smaller, submicron particles that are accelerated to higher speeds. Unless stated otherwise, the experiments described herein were performed with light gas guns.

The first report of successful capture of high-speed particles in aerogel under controlled conditions was by Tsou et al. (1988), with aerogel of density 150 kg m^{-3} and glass beads fired into it at a speed of 5.13 km s^{-1}. They found clear tracks and captured particles in the aerogel. Glass beads of 50 μm diameter left tracks approximately 1.5 mm long. They also found observable tracks from particles as small as 10 μm. In a second paper (Tsou et al. 1989), the same group showed that a 1.6-mm-diameter aluminum sphere could be captured relatively intact in aerogel of density 50 kg m^{-3}. The track length was given as of order 20 cm and at 5–6 km s^{-1}, only some 60% of the original particle's mass was recovered in a single object at the end of the track.

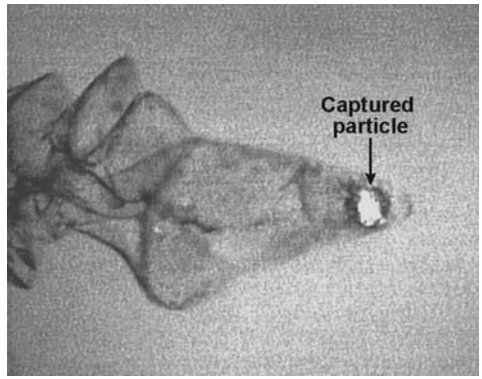

Figure 3

Captured particle. Particle size is 187 microns. Aerogel density was 60 kg m^{-3}, and impact speed was 4.9 km s^{-1}. The impact was from left to right.

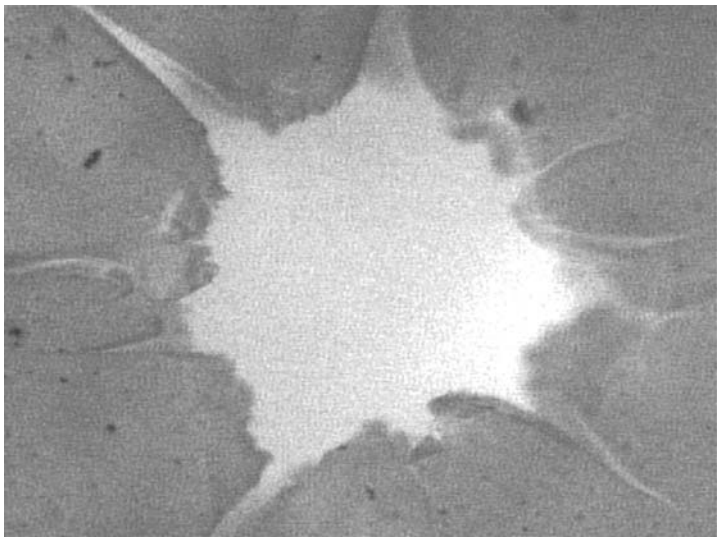

Figure 4

Entrance hole in aerogel (density 60 km g^{-3}). The average diameter of hole was 1.2 mm, particle size was 187 microns, and impact speed was 5 km s^{-1}. At lower densities, circular holes with no lateral cracks are found.

These early experiments demonstrated the feasibility of capture in aerogel. It was then quickly established that track length increased both with impact speed and as the aerogel density was reduced (e.g., Zolensky et al. 1989, 1990).

Hörz et al. (1992) compiled data from the literature on track length in aerogel and other porous media and again observed that track length was inversely proportional to target density. This was confirmed by Barrett et al. (1992) who suggested that at fixed speed, track length increased with projectile density (e.g., with energy). They also noted that track length was relatively insensitive to changes in impact speed from 5 to 7 km s^{-1}.

Using aerogels of density 96 kg m^{-3} and impact speeds of typically 5.3 km s^{-1}, Burchell & Thomson (1996) and Burchell et al. (1999b) reported on capture in aerogel of glass beads and olivine grains (75 to 250 microns in diameter). They found significant scatter (up to 30%) on track length under fixed impact conditions. Similar reports have been given by others, suggesting this is a typical feature of capture in aerogel. They reported that particles typically penetrated into the aerogel to a depth of 80 $\pm$ 20 times particle diameter. They found that the diameter of the captured grains was 70 $\pm$ 20% of their original diameter, i.e., about only 34% of the original mass was retained.

As well as a quantitative analysis, Burchell & Thomson (1996) gave a qualitative report on their impacts. They noted that some tracks were two pronged and in some cases (10%) they were many pronged. These latter tracks are much shorter than expected and were labeled starburst impacts. Both types of tracks indicate that a substantial disruption and splitting of the particle can occur during the capture process. For two-pronged tracks, the tracks separated deep inside the aerogel, but in the starburst events, the fragments seem to split away from each other at the surface. This provides evidence that even though it is impacting a low-density material, the projectile undergoes a significant shock at the moment of impact.

Early reports of capture in aerogel made reference to the observation that the tracks were gently curved. This could in turn lead to an uncertainty of order 20° in the preimpact direction of flight. This caused concern that even if all other properties of an impact were known, it would not be possible to reconstruct the impact direction with great precision. However, Burchell et al. (1999b) demonstrated that where single-pronged tracks were found (the majority of cases), the initial angle of impact could be obtained from the observed track to within $\pm 2^\circ$. They found that most of the curvature in any tracks was located in the last 10% of the track length, and thus use of the first half of the track length was sufficient to predict the impact direction. Furthermore, for impacts under similar conditions except angle of incidence, the track length did not show any dependence on impact angle. Similar results and conclusions concerning inclined impacts were reported by Hörz et al. (1998). In their work, Hörz et al. also used fine-grained powders as projectiles to simulate impacts by low-cohesion projectiles. From what was probably one of the most extensive shot programs to that date, they concluded that although aerogel was a good capture medium, it was not, in general, possible to determine the detailed impact conditions (particle size at impact, impact speed, etc.) from observations of the captured particle and its associated track in the aerogel.

Not all particles in space are going to be cohesive or have low-volatile content. Evidence from stratospheric dust collections suggests that some of the most interesting, primitive materials may be delicate fluffy clusters of submicrometer domains. One class of particle of particular interest is the icy grains. These may be freshly emitted from a comet nucleus, and are likely to have been encountered during the Stardust encounter of comet P/Wild-2 (see below). Although ice sublimation rates mean small ice grains will not last long after ejection from a comet nucleus at 1.86 AU (as in the Stardust encounter), a 1 mm grain will survive up to 700 s (shrinking as it does), potentially impacting the Stardust aerogel. Yano et al. (1999) performed high-speed ice impacts on aerogel. There has been little experimental work on firing ice grains at speeds of many kilometers per second (although ice firing guns were developed in the 1990s for firing ice pellets into tokamak experimental fusion apparatus at speeds of 2 to 4 km s^{-1}). Accordingly, Yano et al. (1999), fired nylon projectiles at solid ice targets, allowing the ice ejecta to then impact their aerogel samples. They reported that ice ejecta hit their aerogels (density 30 kg m^{-3}) at speeds of up to 2.8–3.6 km s^{-1}. Short tracks/shallow pits were observed in the aerogel with no particles at their ends (as might be expected when the ice has melted/vaporized during capture).

A program of impacts in aerogels at speeds reaching up to 14 km s^{-1} was reported by Kitazawa et al. (1999). They fired glass, olivine, and Al_2O_3 particles (10–400 microns in diameter) at aerogels of density 30 kg m^{-3}. To achieve speeds above 5 km s^{-1}, they used a plasma gun, where a metal foil is rapidly heated and explodes as a result of passage of a current through it. This takes place in a magnetic field, and the force from the current flow in a B field, combined with the pressure from the explosion products, accelerates a plasma jet. This is directed through a body of projectiles that are accelerated by the plasma dragging them along with it. Streak cameras identified impact sites on the aerogel, and their associated impact speeds were found

by observing the impact induced light flash. A thin (0.4–0.6 micron) Mylar film in front of the aerogel provided particle size data just before impact. They found that the normalized track length (track length/projectile diameter) fell as impact speed increased. They did not perform a detailed analysis of their data, but at 5 km s^{-1} the normalized track length was approximately 200, albeit with significant scatter on the data. This can be compared to the findings of Burchell et al. (1999b) (see above), who at similar speed reported a normalized track length of about 80 $\pm$ 20 (glass, olivine, and iron projectiles). The difference can be accounted for by the difference in aerogel density, 30 kg m^{-3} (Kitazawa et al. 1999) and 92 kg m^{-3} (Burchell et al. 1999b). Thus a factor of 3 decrease in aerogel density increased the track length by approximately two and a half times.

The relation between track length, projectile size, and aerogel density can be considered by plotting normalized track length (track length/projectile diameter) versus aerogel density (see **Figure 5**). This uses the results quoted above from Tsou et al. (1988, 1989), Burchell & Thomson (1996), Burchell et al. (1999b, 2001), and Kitazawa et al. (1999) for speeds of 5 to 6 km s^{-1}, and projectile sizes from order 100 microns to 1 mm. The particles were composed of minerals, soda lime glass, aluminum, and iron. Despite the diverse range of projectile parameters, the data show remarkably little scatter. **Figure 5** includes two fits to the data, linear and quadratic, but in the range of the aerogel density used there is little difference between the two. Preliminary new results from Foster (2006) suggest that both fits significantly underestimate the normalized track length at an aerogel density of 13.5 kg m^{-3}. Using 22 micron diameter glass beads impacting at 6.1 km s^{-1}, Foster (2006) finds a normalized track length of 500–600, more than twice that predicted here from the quadratic fit. This implies longer than expected tracks in the Stardust aerogels (although, because the Stardust aerogels are of density varying with depth, track length is hard to predict). At high densities, the linear fit also appears to fail, as it predicts zero track length at aerogel density 186 kg m^{-3}. This point is returned to below.

While **Figure 5** suggests a simple relationship giving track length as a function of projectile size and aerogel density, it must be remembered that this is in a narrow range of impact speed. The influence of impact speed on track length is illustrated by Burchell et al. (2001). Using three aerogel densities (60, 96, and 180 kg m^{-3}), they reported data for impacts of spherical glass beads (diameter 106 $\pm$ 2 microns) at speeds of 1 to 7.5 km s^{-1}. They again found that track length was inversely related to aerogel density. However, they also found that track length did not continually increase as impact speed increased. Instead, as impact speed increased, track length initially increased, then reached a maximum, and finally started to fall. This is shown in **Figure 6*a***. The impact speed v_{max}, where track length was a maximum, varied inversely with aerogel density ρ. Burchell et al. (2001) could not distinguish between a linear or a power law fit to the relationship between v_{max} and ρ and offered two solutions:

$$v_{max} = 7.33 - 0.021\rho \quad (1)$$

$$v_{max} = 45.4\rho^{-0.49} \quad (2)$$

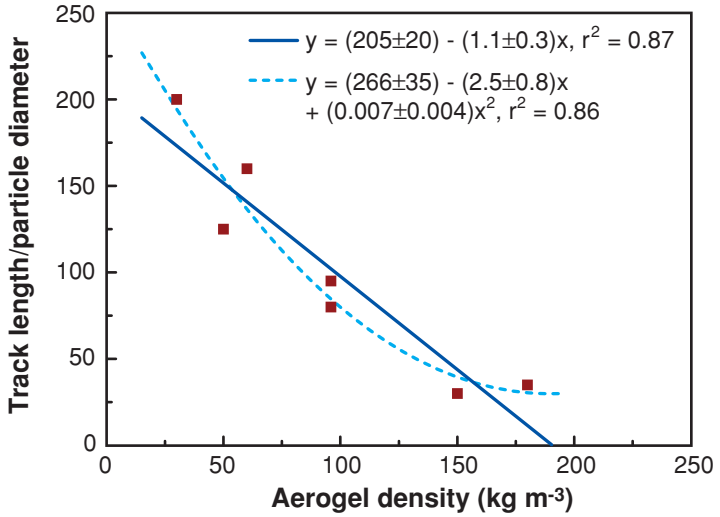

Figure 5

Normalized track length versus aerogel density for impact speeds 5–6 km s^{-1}.

where v_{max} is in km s^{-1} and ρ is in kg m^{-3}. These two solutions diverge significantly at lower densities (see **Figure 6*b***) and more data is needed to find the correct behavior.

Kitazawa et al. (1999), also reported on entry hole diameter. They found that this scaled with projectile diameter, and ranged from 5.6 to 9 times the projectile diameter. It should be noted that their data had a large scatter about these mean values, and included some highly oblique impacts [even though Burchell et al. (1999b) showed that entrance holes in such cases are no longer circular]. The maximum track width observed by Kitazawa et al. occurred below the aerogel surface and was some 11.3–14.3 times the projectile diameter. This result was given independent of impact speed. Using only normal incidence impacts, Burchell et al. (1999b) found that for glass and olivine particles of 100 microns diameter, the entrance hole was 1.97–2.2 times projectile size, falling to 1.2–1.9 times projectile diameter for particles of 300 microns. Again, this difference in scale can be associated with the difference in aerogel density. Thus, larger entrance holes and track widths are found in lower density aerogels.

Burchell et al. (2001) found that the entrance hole diameter was well approximated by the particle diameter below 2 km s^{-1}, and above this it rose linearly with impact speed, with a more rapid increase the lower the aerogel density. Above 2 km s^{-1}, they found that the entrance hole diameter could be fit by the linear equation $a + bv$ (where v is impact speed), where, if v is in km s^{-1}, the slope b (dimensionless if hole size and projectile diameter are in the same units) can be given in terms of aerogel density by:

$$b = 2.56 \times 106\rho^{-2.33}. \quad (3)$$

The value of the intercept a depends on projectile diameter (d) and the coefficient b. From the data of Burchell et al. (2001), we obtain

$$a = d - 2b, \quad (4)$$

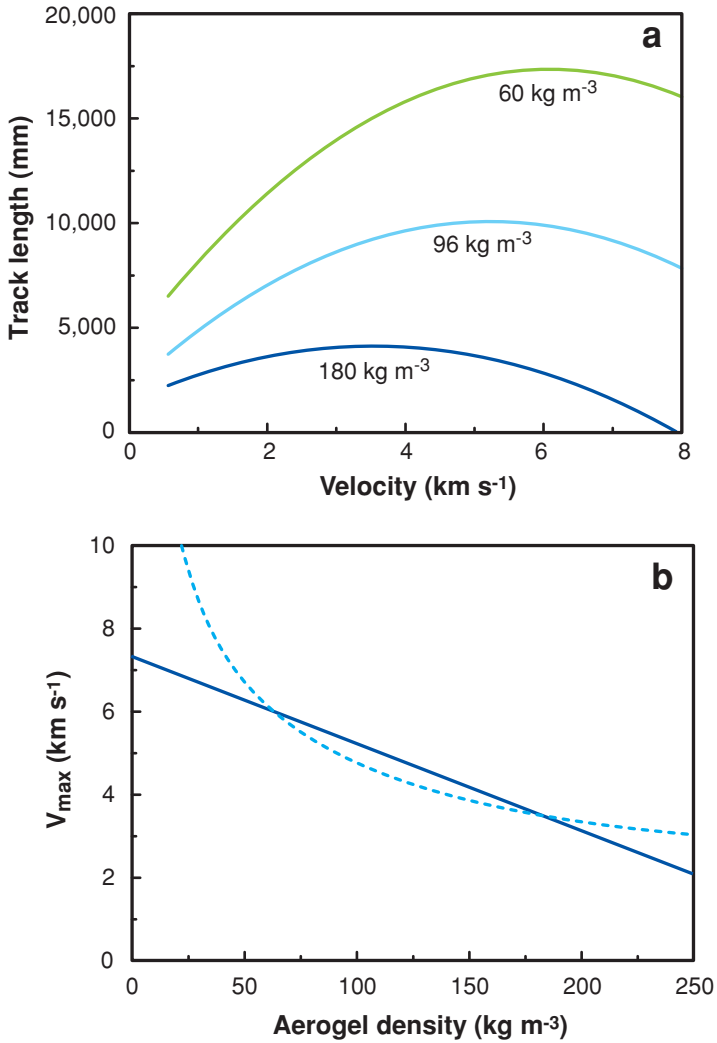

Figure 6

(*a*) Track length versus impact speed for different aerogel densities. (*b*) Impact speed (v_{max}) at which track length is a maximum versus aerogel density.

where the impact speed is in km s^{-1}, aerogel density in kg m^{-3}, and projectile and hole diameters are in microns. The dependence of hole size on impact speed implies that averaging data over a speed range of 1–14 km s^{-1}, as done by Kitazawa et al. (1999), can be expected to introduce a strong bias to the data.

Kitazawa et al. (1999) also reported that the volume (V) excavated by a track could be given in terms of impact kinetic energy (E) by

$$E = 1000V^{0.56}, \quad (5)$$

where V is in m^3 and E is in J (ranging from 10^{-4} to 1 J). Burchell et al. (2001) also included a parametrization of the excavated track volume arising from impacts of

Figure 7

Track volume versus impact kinetic energy.

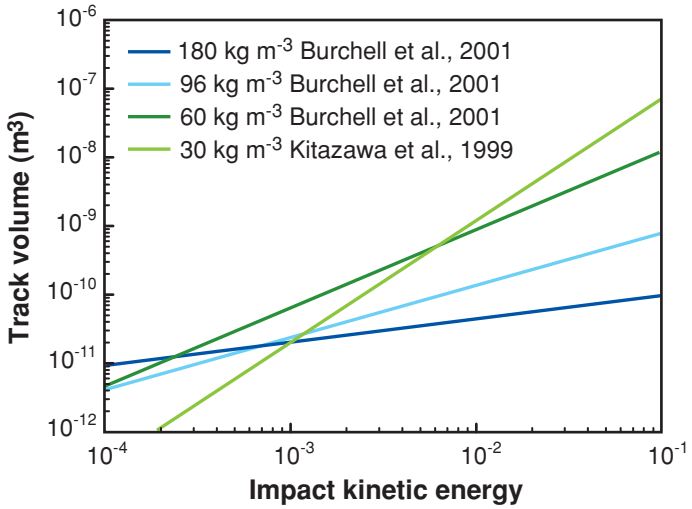

106 micron glass beads, and did this at three aerogel densities (60, 96, and 180 kg m^{-3}). A fit of the form

$$V = A \times E^{B} \tag{6}$$

was performed at each aerogel density. The results are shown in **Figure 7** along with the equivalent result from Equation 5. It was observed that both coefficients A and B depended on aerogel density, and that, in general, track volume was inversely correlated with aerogel density, although at low energies the results from Kitazawa et al. (1999) contradict this. Ignoring this inconsistency, a combined fit of the form of Equation 6 can be made to the results of Kitazawa et al. (1999) and Burchell et al. (2001). This gives

$$A = (26 \pm 13)\rho^{-(4.76 \pm 0.08)} \tag{7}$$

$$B = 7864\rho^{-(6.0 \pm 1.4)}, \tag{8}$$

where ρ is in kg m^{-3}. No uncertainty is given on the scale coefficient for B as the fit was relatively insensitive to variations in this parameter. In principle, use of Equations 7 and 8 to obtain the coefficients A and B for Equation 6 permits an estimate of track volume at all aerogel densities and impact energies. However, this has been obtained from a relatively limited set of impact conditions.

The text above refers to relatively large dust particles (tens of microns to millimeter scale). Impacts by micron-sized particles have also been observed in the laboratory (using Van de Graaff accelerators). Tsou et al. (1990) observed impacts of iron dust into aerogels of density 60 kg m^{-3} at speeds of a few to 15 km s^{-1}. Later, Burchell et al. (1999a) used a similar Van de Graaff accelerator but selected the iron particles in flight and only directed those in narrow (1 km s^{-1} breadth) speed bands (and thus restricted size ranges) onto the target aerogel. However, although the experiments were reported, in both cases there was very little numerical data presented. Nevertheless, these experiments do suggest capture is feasible even for micron-sized particles.

TRACKS OR CRATERS AS AEROGEL DENSITY INCREASES?

Impacting particles leave tracks in low-density aerogel, but as the aerogel density is increased, the tracks shorten in length and eventually become craters. In **Figure 5**, the linear fit suggests that for impacts at 5–6 km s^{-1}, tracks vanish at an aerogel density of 186 kg m^{-3}. The tracks presumably become so short that they effectively appear to be shallow pits/craters rather than tracks. One report of cratering under impact (rather than penetration and track formation) is that of Tedeschi et al. (1995). For a single shot of a 2.39-mm-diameter aluminum projectile at an impact speed of 7.58 km s^{-1} into aerogel of density 224 kg m^{-3}, they reported an impact crater rather than a track. However, the crater reached to the sides and almost to the bottom of the target holder and complex extensional shock wave from the boundaries may be involved. This experiment may thus not give the definitive result as to the aerogel density where the track versus cratering limit lies. In general, tracks are observed in aerogels of density around 200 kg m^{-3}. Foster (2006) reports that for impacts at 5 km s^{-1}, if aerogel density exceeds 200 kg m^{-3} then glass projectiles appear to break up during impact, producing multiple short tracks, and for aerogels of >300 kg m^{-3} only shallow, pit-like craters are observed. An aerogel density of around 200 kg m^{-3} thus appears to be the boundary between tracks or cratering at these speeds. More work is required on this issue and the threshold may be velocity dependent, for example.

PASSIVE VERSUS ACTIVE CAPTURE IN AEROGEL

One drawback of the use of aerogel as a dust collector in space is the passive nature of the collection. This means that, for example, there is no timing information as to when a particular capture event occurred, nor any measure of impact speed, etc. The NASA Stardust mission (see below) has constrained timing and velocity issues by capturing cometary dust during a brief passage near a comet nucleus at an impact speed almost totally determined by the well-calibrated fly-by speed of 6.1 km s^{-1}. However, even the Stardust mission lacks time and velocity calibration during its capture of interplanetary and interstellar dust, when the aerogel collectors were left exposed for lengthy periods and the impact speeds were unknown. One technique to overcome some of these limitations is that of adding electronic sensors to the aerogel. To this end, McDonnell et al. (2000) proposed adding microphones to aerogel blocks. Several such microphones could act to triangulate an impact on a block providing a time-sensitive flux measurement. In addition, based on the magnitudes of the measured signals and the attenuation distance from impact to microphone, the impact momentum could be established, which combined with estimates of particle mass after later laboratory examination, could provide an estimate of impact speed. However, this remained at more of a proof of concept stage than detailed calibration data for a specific device. Indeed, it should be noted that the acoustic properties of aerogel do not follow those for homogeneous materials or classical theory for porous materials (Gibiat et al. 1995) and that propagation of shock signals from impact should be determined experimentally. Data for response of aerogels to shock compression

ISS: International Space Station

(i.e., shock velocity and equation of state from Hugoniot data) have been obtained (e.g., see Holmes & See 1992 or Grover et al. 1992). However, for any given configuration of aerogel and microphones proposed for use in space, a full calibration program would be required. Development of piezoelectric impact detectors on the aluminum structural framework of the aerogel-carrying the Large Area Debris Collector (LAD-C), to be deployed on the International Space Station (ISS), will have to address this problem.

Auer (1998) reported an impact ionization experiment using aerogels. It was hoped that this technique could help produce an independent measure of impact speed for a captured particle (although how to subsequently associate individual tracks in the aerogel with specific ionization signals was not established). A Van de Graaff accelerator was used to accelerate iron dust with diameters from 10 to 0.1 μm. This corresponded to speeds of 1 to 80 km s^{-1}, respectively. Impact ionization was observed and the specific charge (charge/mass) correlated with impact speed. At low speeds, although detectable, the ionization charge was up to two orders of magnitude less than that from similar impacts on thick metal targets, and at speeds above 50 km s^{-1}, the charge was still typically 1 order of magnitude less than that for impacts on metals. Considerable scatter was found on the data as is typical for impact ionization experiments, meaning that speed determinations are usually limited to, at best, a factor of two in accuracy at high speed. So the technique seems of limited use.

Another approach to obtaining extra information about the impact event in aerogel is to use the aerogel to record the extra information. A novel example of this concerns alumina aerogels doped with chromium(III) (Domínguez et al. 2003). The amorphous phase of this aerogel is only weakly fluorescent, but if the aerogel is heated above 1450°C, it undergoes a permanent phase transition to a strongly fluorescent state. When a particle impacts the aerogel at high speed, it deposits energy along the track and the resultant heating can be sufficient to trigger this phase change. The volume of aerogel affected is related to the impact energy. Thus subsequent measurement of the fluorescent properties of the aerogel track gives a signal proportional to the impact energy. It is proposed that this can then be used to indicate possible differences in impact speed for captured particles and hence give clues as to their origin.

PARTIALLY INTACT CAPTURE AND MODIFICATION DURING CAPTURE

Although aerogel is widely held to capture high-speed particles intact, this is not strictly the case. A more correct description would be that of relatively intact capture. The report by Tsou et al. (1988) refers to intact capture of glass beads, but soon afterward the recovered mass for an aluminum projectile captured in aerogel was quantified as being only 60% to 70% of the original mass (Tsou et al. 1989).

In two papers (Zolensky et al. 1989, 1990) it was reported that mineral grains (initially 1 mm aggregates, but in the later paper monomineralic grains of fosterite, pyrrhotite, and calcite approximately 100 μm diameter) were fired into aerogels of density 20 to 120 kg m^{-3}. Impact speeds were 5, 6, and 7 km s^{-1}. Some alteration of

the captured mineral samples was found along with reduction in mass, but in all cases crystalline domains remained, and for pyrrhotite there was virtually intact capture. However, it was noted that in some cases, particle melting occurred, that rims of mixed aerogel and melted particle formed around the captured particles, and that some loss of volatile components from the projectiles took place.

The issue of how much of a particle was captured and to what degree it was altered during capture was considered by Bunch et al. (1991). They fired a variety of mineral grains into aerogel of density 100 kg m^{-3} at speeds up to 5.6 km s^{-1}. At the highest speed they found that captured grains had suffered a reduction in size, but assigned this to the acceleration during firing and grain-grain collisions in flight such that particle mass was lost preimpact. It is thus important in such work to know the size distribution at impact and not prelaunch. They also reported that a variety of rims (composed of melted aerogel) had formed around the grains. In some cases (e.g., olivine) there was another rim of particle fragments and melted aerogel on the surface of the particle itself. But even at the highest speeds, unaltered cores were again found for the captured particles. Nevertheless, some surface heating and alteration (fragmentation at least) had occurred during impact.

Barrett et al. (1992) found similar results and reported that particle residues were seen along the length of the tracks in the aerogel, indicating that the walls of the track should also be considered during analysis. In some cases they reported severe processing of minerals as a result of capture in the aerogel. A study of the captured grains (by transmission electron microscopy) indicated aerogel rims were present on the captured particles that had undergone varying degrees of damage and surface alteration depending on the particle composition, including, for example, extensive ablation, fracturing of the samples, and some evidence of dehydration and reordering. Further, it should be noted that only fairly rigid projectiles were used, as the shock of launch in a light gas gun can cause disintegration of some minerals (e.g., calcite) and fluffy aggregates cannot easily be accelerated. Hörz et al. (1998) showed that for a wide range of projectiles (soda lime glass, aluminum, Allende meteorite, etc.) of size 50 microns impacting low-density aerogels (10 to 50 kg m^{-3}) at 6 km s^{-1}, the captured particles ranged in size from 30%–95% of the diameter of the original, with all experiencing some mass loss. Burchell et al. (1999b) reported that for impacts of soda lime glass, olivine, and iron at 5.3 km s^{-1} into aerogel of density 92.5 kg m^{-3}, the captured mass fraction was typically 60%–80% for 100 micron-sized particles, and showed evidence of falling to 20% as particle size increased to 300 microns. This suggests that capture in aerogel is more effective for smaller particles.

The speed dependence of the mass loss during capture was illustrated by Kitazawa et al. (1999), who showed that at speeds of 1 km s^{-1}, soda lime glass, olivine, and aluminum oxide particles were captured intact in aerogel of density 30 kg m^{-3}. This changed as impact speed increased, such that at 6 and 10 km s^{-1}, the captured particles were typically only 0.7 ± 0.2 and 0.5 ± 0.2 times the original particle diameter, i.e., on average only 34% and 12.5%, respectively, of the original mass was captured at the end of the track.

This dependence on impact speed was also studied by Burchell et al. (2001), who reported data for soda lime glass beads (preimpact diameter 106 microns) impacting at

1 to 7.5 km s^{-1} into aerogel of density 60 to 180 kg m^{-3}. They again found that 100% of the particle was captured at 1 km s^{-1}, but that this fell as impact speeds reached 5–6 km s^{-1}. However the captured particles still typically had diameters over 90% of their preimpact size even at 7+ km s^{-1} for all the aerogel densities used in their work.

In a study of alteration of hydrated mineral grains (serpentine and cronstedtite) during capture in aerogel (30 kg m^{-3}) at 2–4 km s^{-1}, Okudaira et al. (2004) stated that the captured volumes were only 10% of the original grain volume. However, this was obtained by assuming that the grain size at impact was given by the entrance hole size in the aerogel and comparing this with the volume of the captured grains. Because earlier work had shown that the entrance hole was typically larger than the impacting grain, this must be suspect. In a later report (Okudaira et al. 2005), the same authors estimated that at 6 km s^{-1}, between 10% and 100% of the incident particle was captured intact in the aerogel. In both cases (Okudaira et al. 2004, 2005) a mineralogical analysis of the captured grains was carried out. They found that there was no anhydrous decomposition of these hydrated minerals. For both types of minerals, there was evidence of surface heating, resulting, for example in the case of one serpentine grain, in an amorphous layer around a still crystalline core. For the cronstedtite, a mixed mineral:aerogel rim was observed, apparently formed from a molten state. However, even as little as 150 nm below the rim, the chemical composition of the grain was unaltered. This confirms earlier observations (e.g., Bunch et al. 1991), but even with these changes, it should be noted that unaltered regions were again found in all recovered grains.

MODELING OF CAPTURE MECHANISM

Modeling of capture in aerogel based on first principles is still at a basic level. Such work tends to be based on an approach similar to that of Anderson & Ahrens (1994), who developed a three-component model for capture in foams (which are also mesoporous materials). Their model simulated capture in a low-density medium, which dissipated the impact energy over a relatively large length such that the particle was captured relatively intact. The model included contributions from drag, ablation, and fragmentation, and it assumed that particle size was greater than the cell size in the foam. However, Anderson & Ahrens noted that changing the target from an organic foam to an inorganic material, such as aerogel, might significantly alter the relative contributions of the different components in their model, so their results for foams cannot simply be applied to all similar low-density materials.

A simple model for impacts into low density objects was proposed by Kadono (1999). In this work, laboratory data for impacts in low-density foams and aerogels was used to develop equations to parameterise track lengths and volumes in the capture media. These were then explained in terms of physical impact processes, including disruption and fragmentation of the projectile. The results were then applied to the larger-scale case of asteroids hitting comets, but could presumably be applied back to the original case of dense objects impacting aerogel.

A more recent model of compaction-driven capture in aerogel was proposed by Domínguez et al. (2004). They compared their model to laboratory data and found

that it was difficult to account realistically in the model for the differing contributions to the slowing down of the captured particle by projectile ablation versus accretion of molten aerogel onto the particle. This prevented a detailed understanding of the slowing mechanism and prediction of track length. However, they were more confident in understanding the entrance hole radius in terms of attenuation of a sideways expanding cylindrical shock wave.

Mir: Russian space station in LEO 1986–2000

In none of the above cases is a fully developed model presented that fits the known behavior and data for capture in aerogel. There is clearly more work required to fully understand the complicated interplay of physical mechanisms at work in high-speed capture of particles in aerogel.

USE IN SPACE

Even before it had been demonstrated that aerogel could capture particles in high-speed impacts, aerogel dust collectors were already deployed in space. Initially flown on the space shuttle several times, aerogel collectors were then flown on a retrievable satellite (EuReCa), on the outside of the Mir space station (several times) on missions into interplanetary space (Stardust) and on the outside of the ISS.

The first use of aerogel in space was on space shuttle flights STS 41-B, STS 41-D, and STS-61B in 1984/85 (Maag & Kelly Linder 1992). A common particle capture experiment (consisting of organic foams, aerogel, and kapton foil) was used. The aerogel in STS 61-B captured an aluminum oxide sphere (probably from the exhaust of a solid rocket motor).

Later (in 1992) STS-47 also carried aerogel capture cells (density 20 kg m^{-3}). After 170 h exposure time, the aerogel was examined on Earth and found to contain four hypervelocity impact tracks (Tsou et al. 1993). Although only an optical analysis was carried out, based on the characteristics of the tracks and particles, three of the four were tentatively identified as silicate in origin, with the fourth as man-made space debris. This is thus probably the first successful capture of extraterrestrial dust in aerogel in space. Similar cells were also flown on STS-57, STS-60, STS-64, and STS-68 (Tsou 1995).

This was then followed by deployment of an aerogel collector on the European Space Agency's retrievable satellite EuReCa. The Ticce experiment contained four aerogel trays (0.04 m^2 of 50 kg m^{-3} aerogel) and was exposed in space for 11 months. Analysis on the ground revealed 10 tracks and two bowl-shaped pits in the aerogel (Brownlee et al. 1994). Subsequent discussion of the impact conditions indicated a likely source for the extraterrestrial particles to be micrometeoroids with retrograde trajectories (Burchell et al. 1999b).

Several experiments on the exterior of the Mir space station involved deployment of aerogel dust collectors. The Euro Mir '95 experiment was exposed from October 1995 to February 1996. Examination of its two aerogel (density 100 kg m^{-3}) collectors back on Earth offers a cautionary tale (Shrine et al. 1997). One aerogel sample had broken up, apparently owing to a mechanical shock either from handling during retrieval or handling on the ground. The other showed no sign of impacts of particles (lower size limit microns), and flux models subsequently predicted only two such

impacts were likely during its exposure. This illustrates that the brittle nature of aerogel requires special handling procedures and that exposures of short times or small surface area (i.e., a low area:time product relative to the expected flux) are of limited value.

ODC: Orbital Debris Collector (experiment deployed on the Mir space station)

MPAC: Micro-particles Capturer

DFMI: dust flux monitor instrument (on the Stardust spacecraft)

CIDA: cosmic and interstellar dust analyser (instrument on the Stardust spacecraft)

More successful was the deployment of 0.63 m^2 of aerogel (20 kg m^{-3}) on the exterior of Mir for 18 months as part of the Orbital Debris Collector (ODC) in 1996–1997 (Hörz et al. 2000). Hundreds of impacts were found during the subsequent analysis, some of which featured in-clusters (where it was assumed a primary impact on a nearby surface of Mir produced a swarm of secondary ejecta which then impacted the aerogel). Based on their depth (t) to diameter (D) ratios, the impact features were classified as tracks ($t/D > 10$), pits ($0.5 < t/D < 10$), or shallow depressions ($t/D < 0.5$). The pits were not analogous to any laboratory impacts and were held to arise from ultra-fast impacts. They contained no identifiable captured particle and little in the way of impact residues. The shallow depressions were in two main classes: one where flakes of material were stuck in the aerogel, probably from very-low-speed impacts, and the others were dish-shaped depressions, probably from low-speed liquid impacts. In general, these shallow depressions were considered to arise from contaminants from the Mir environment itself, hence their low impact speed.

Recently, aerogel dust collectors have been deployed on the exterior of the ISS. For example, the Japanese experiment MPAC (Micro-Particles Capturer) deployed three units on the ISS in 2001 (Kitazawa et al. 2004). One was retrieved after 315 days exposure in 2002, the second was retrieved in 2004, and the third will be retrieved later. The aerogel in each unit consisted of 48 tiles (each 37 × 37 mm and 15 mm thick) of density 30 kg m^{-3}. The number of features observed during analysis of the first retrieved unit exceeded expectations based on flux models by factors of 5 to 100, depending on particle size. This was attributed to a failure of the flux model used, contamination from the ISS environment and approaching vessels, or from secondary ejecta from impacts on nearby surfaces. It is clear from the experiences of both ODC (Mir) and MPAC (ISS) that these latter two points have to be allowed for when making flux measurements based on counting impacts in aerogel. Further, if the flux model used with the MPAC analysis was not in error, then it seems these contaminants (man-made debris from the local environment) or showers of ejecta from nearby surfaces may significantly dominate the captured particles in aerogel deployed in LEO.

STARDUST MISSION

One of the major current uses of aerogel in space is the dust particle collection system on board the NASA *Stardust* spacecraft. The Stardust mission (Brownlee et al. 2003) was launched in February 1999, with the intention of flying past comet P/Wild-2 in January 2004 and returning captured dust samples to Earth in January 2006. The spacecraft carries several instruments for the characterization of cosmic dust. A real time dust flux monitor (DFMI) (Tuzzolino et al. 2003) electronically recorded impacts of small particles on the spacecraft's main bumpershield. An impact ionization detector combined with a time of flight ion mass spectrum analyzer CIDA [cosmic

and interstellar dust analyser (instrument on the *Stardust* spacecraft)] (Kissel et al. 2003) was operational during the mission and encounter. The final major instrument was a passive dust collector using aerogel as the capture medium (Tsou et al. 2003). With a planned cometary encounter speed of 6.1 km s^{-1}, the capture process in aerogel was well matched to laboratory experiments that have demonstrated the feasibility of capture at such speeds (see above).

SEM: scanning electron microscope

The DFMI instrument was active during the cometary encounter in January 2004, and based on its data, it is predicted that the aerogel was impacted by 2800 $\pm$ 500 particles of 15 micron size or above (Tuzzolino et al. 2004). The largest-sized particle statistically likely to have hit the aerogel was predicted to be of order 1 mm. Such a particle would not be retained by an aerogel block of the size and density deployed on Stardust, and may indeed have destroyed a single block with its impact. There is, however, some uncertainty on these predicted flux numbers, as the CIDA instrument returned far less data (Kissel et al. 2004) than anticipated based on the DFMI flux results. This raises the possibility of a lower flux in the aerogel as well.

The *Stardust* aerogel consists of 160 sections mounted in a grid like arrangement on a deployable arm. The aerogel is unusual in that it does not have a single uniform density, instead there is a density gradient through each block as one goes from the surface (low density) to the interior (higher density). This means particles encounter the lowest density while at the highest speed and then encounter the higher density as they slow down. Another feature of the aerogel collector is that both front and rear faces can be exposed to space, and both faces have their own layers of aerogel blocks. During the cometary encounter, the front face was pointed at the comet to collect the freshly emitted cometary dust grains. At other times during the cruise between launch and cometary encounter, the aerogel was deployed such that interplanetary or interstellar particles would preferentially impact the rear face. The aerogel blocks facing frontward and rearward are placed back to back in the collector frame. The cometary dust-collecting (frontward-facing) blocks have a front surface density of 5 kg m^{-3}, rising to 50 kg m^{-3} at the rear of the block. The rearward-facing blocks have a front face density of 5 kg m^{-3}, rising to 20 kg m^{-3} at their rear face.

The aerogel blocks are mounted in their frame under tension, using aluminum foil to hold them in place. This foil can be used to remove the blocks from the paddle after the aerogel is returned to Earth. Each separate block will then be available for analysis, as will be the foil. The latter point is significant, as the foil will have some of its surface exposed to impacts and will retain impact craters whose diameters will be resolvable to below 1 micron [under scanning electron microscope (SEM) analysis]. Such craters will be made by particles about four times smaller in diameter than the crater. This will complement the flux measurement made using the tracks found in the aerogel and extend it to sizes (submicron) where it is assumed the aerogel analysis will not provide information. It may also be possible to obtain some dust compositional information from the residues found in the craters (Graham et al. 2003, Kearsley et al. 2005).

The returned Stardust aerogel and dust samples will be held by the NASA JSC Curatorial Facility at Houston and will be available for analysis (Zolensky et al. 2004). Excluding the more tenuous solar wind samples provided by the Genesis mission,

these will be the first significant returned Solar System samples collected away from Earth by NASA since the Apollo era.

IN SITU ANALYSIS TECHNIQUES

Beyond optical measurement of the tracks and particles captured in the aerogel, the main goal of analysis studies is to determine particle composition. Because aerogel is optically transparent, locating captured particles is straightforward. The particles can be examined in situ without the need for removal by a variety of means. A detailed discussion of how to analyze nanogram samples in general is given in Zolensky et al. (2000). Two methods particularly relevant to in situ analysis are synchrotron X-ray fluorescence and Raman spectroscopy.

Synchrotron X-ray fluorescence was demonstrated on samples of Allende carbonaceous chondrite fired in aerogel (density 20 kg m^{-3}) at 3 to 6 km s^{-1} (Flynn et al. 1996). An X-ray microprobe at the Brookhaven National Laboratory (U.S.) provided an 8-micron-diameter X-ray beam. The X-rays excited in the target sample were able to escape from depths inside the aerogel of up to 5 mm. Elements such as Ca, Ti, Cr, Fe, Ni, Cu, and Zn were all detected in the Allende particles. The aerogel itself was found to give signals for Si, Ar, Ca, and Fe. The fluorescence signals were attenuated by passage through the aerogel and the signals from low Z elements were lost first if the particles were behind increasing depths of aerogel. In a later paper (Flynn et al. 2000) it was reported that in low-density aerogel the maximum aerogel depth for analysis was 0.1 mm for Al, a few millimeters for Ca, and several centimeters for Fe. Signals were also observed from the aerogel for Ca, Ti, Fe, Cu, and Zn as well as Si. Subtraction of the signal from an aerogel region away from the particle was thus required when analyzing the particle composition. Overall, when combined with X-ray diffraction studies of the captured particles, the technique is a powerful tool to determine chemical and mineralogical characterization of captured particles. Indeed from characteristic ratios of transition metal elements, Flynn et al. were able to infer that some particles in their study (using aerogel exposed on Mir) were chondritic in composition and thus extraterrestrial in origin. However, for a more precise mineralogical determination, the differential absorption of different energy X-rays must be taken into account during interpretation of the resulting spectrum.

The second major in situ technique is application of Raman scattering. This uses an incident monochromatic light source inelastically scattered from the sample. The wave number shift of emitted lines in light scattered from the sample reveals detailed information about the bonding structure of the sample and thus its composition. The technique has long been applied to mineralogical studies and the spot size on the sample can be of order a few microns. Its use for identifying mineral grains captured at high speed in aerogel was first illustrated by Burchell et al. (2001). They used olivine and enstatite grains (size of order 100 μm) captured in aerogel of density 96 kg m^{-3}. Raman spectra from the grains in the aerogel were compared with those from raw grains and gave positive identification of the minerals. As well as Raman scattering, the same experimental conditions may also produce visible wavelength fluorescence from suitable materials. These characteristic fluorescent signals can also be used to

identify minerals, as was also demonstrated for ruby and spinel by Burchell et al. (2001).

Since then, the same group has demonstrated that Raman and fluorescence analysis can be successfully applied for a wide range of minerals captured in aerogel (e.g., albite, calcite, corundum, enstatite, lizardite, nepheline, and rhodonite). Such wide applicability emphasizes the value of Raman techniques. Burchell et al. have also shown that inhomogeneous meteorite samples (Allende, Murchison, Orgueil) can be fired into aerogel and Raman techniques used to identify components such as olivine and enstatite. It should be noted that Raman analysis is not limited to identification of minerals alone (although it does not work on all materials). Burchell et al. (2006) have shown that Raman signals for carbon can be obtained from samples fired into aerogel. This can be used to flag a possible organic content of captured grains. And again, using Raman techniques Burchell et al. (2004) demonstrated positive identification of two organic materials; poly(methyl methacrylate), PMMA, and poly(ethyl methacrylate), PEMA, after their capture in aerogel from a light gas gun shot.

One possible drawback of using Raman techniques on grains in situ within aerogel lies in the heating effect of the illuminating laser. Aerogel is a poor heat conductor and any particle temperature elevated due to heating by the laser is mostly reduced via radiation and not conduction. This has been studied by Burchell et al. (2006) who found that in most cases the heating is modest (of order 20°C), but that in some cases it can be extreme (several hundred degrees Celsius). Indeed, in unpublished work the group has shown that some materials can suffer ablation and surface pitting owing to the heating effects of the illuminating laser. Hence care is needed when using this technique on very small particles (10 to 20 microns), which are very volatile-rich and good absorbers of laser light.

EXTRACTION METHODS

Successful extraction of particles from aerogel for analysis in the laboratory is an important technical skill. The cost of missions to deploy and retrieve aerogel capture cells in space places a requirement that the samples not be wasted due to poor handling skills. The simplest approach to extraction is to cut the aerogel along the capture track with a scalpel blade. This exposes surfaces that can be analyzed but may not expose the particle or, worse, the particle may be displaced and lost during cutting. Although this works well for millimeter-sized particles, for smaller particles this approach is not appropriate.

A slightly more sophisticated method is to clamp the sample to a support, and using a drill (with narrow-diameter drill bit) excavate a new track leading to the captured particle. Usually this new track is at right angles to the particle track. A probe can then be inserted along the newly drilled track, and using sharp-pointed tools, the captured particle can be extracted. If done under a microscope, after minimal practice, 100% successful extraction of particles of sizes down to 100 microns can be achieved. For smaller sizes more precise methods are required.

One technique to remove small particles from larger samples of aerogel is to isolate the region of aerogel containing the particle and remove the particle intact. One way

to do this is to use laser cutting of the aerogel to expose a small block of aerogel around the desired particle (Graham et al. 2004a). The surface covering is ablated away by the laser and shafts cut around the particle. The region around the particle can then be removed using sharp probes. Precise cutting of aerogel has also been demonstrated by Ishii et al. (2005), who used a joystick-controlled micromanipulator fitted with a high-frequency oscillator and diamond blades.

A more sophisticated approach is to create excavating trenches and tunnels in the aerogel using an automated micromanipulator and glass microtools, and then use silicon microtweezers to remove a small region of aerogel containing the particle, track, and residue (Westphal et al. 2002, 2004). The resulting aerogel "keystones" can be used to isolate particles down to 3 microns in size. They can then be handled in the laboratory or transferred from place to place, providing a robust way to store and carry individual particles and tracks isolated from a larger aerogel sample. Ion beams can also be used to further expose the particles in the keystones by ablation of the remaining aerogel cover on the particles, making the freshly exposed particle surfaces available for analysis (Graham et al. 2004b).

FIB: focused ion beam

TEM: transmission electron microscopy

STEM: scanning transmission electron microscopy

FTIR: synchrotron Fourier transform infrared spectroscopy

SEI: secondary electron imaging

ANALYSIS OF EXPOSED/EXTRACTED PARTICLES

Analytical SEM has already proven a very useful tool in the location and examination of materials trapped in aerogel (e.g., Hörz et al. 2000, Graham et al. 2005). The suite of essentially nondestructive imaging and analysis methods that can be supported on a SEM allow rapid examination of broken and cut surfaces of aerogel, and the location of impacting particle remnants in situ within impact tracks and their analysis (Graham et al. 2004b). The use of combined SEM and focused ion beam (FIB) instruments also permits precise sampling of material for extraction and subsequent analysis by methods such as analytical transmission electron microscopy (TEM), scanning transmission electron microscopy (STEM), and synchrotron Fourier Transform infrared spectroscopy (FTIR).

Aerogel is a very good thermal and electrical insulator, with a moderate secondary electron yield from electron beam irradiation. This causes some problems of charge accumulation, creating high contrast in secondary electron images (SEI) across edges and sharp topographic features (**Figure 8**) and often severe image distortion owing to beam deflection. The surface of aerogel will accept a thin carbon coat; however, the pervasive fine-scale porosity and fracture network may prevent efficient grounding. It is also often desirable to avoid sample contamination, especially when later characterization stages may wish to locate and analyze carbon-bearing phases in the aerogel. A greater problem lies in the inability of mounting media to hold aerogel in place on a suitable substrate. Contact with aqueous or alcohol-based adhesives will immediately result in volumetric change in the aerogel, rapidly growing opacity, fracturing, and detachment. Normal adhesive stub surfaces are not usually suitable for mounting aerogel samples, as the very low sample density of the aerogel gives little coupling to the surface below, and it is not possible to "tamp-down" peripheral areas of the sample without causing disintegration. It is similarly difficult to create an effective conductive pathway to the underlying substrate. The

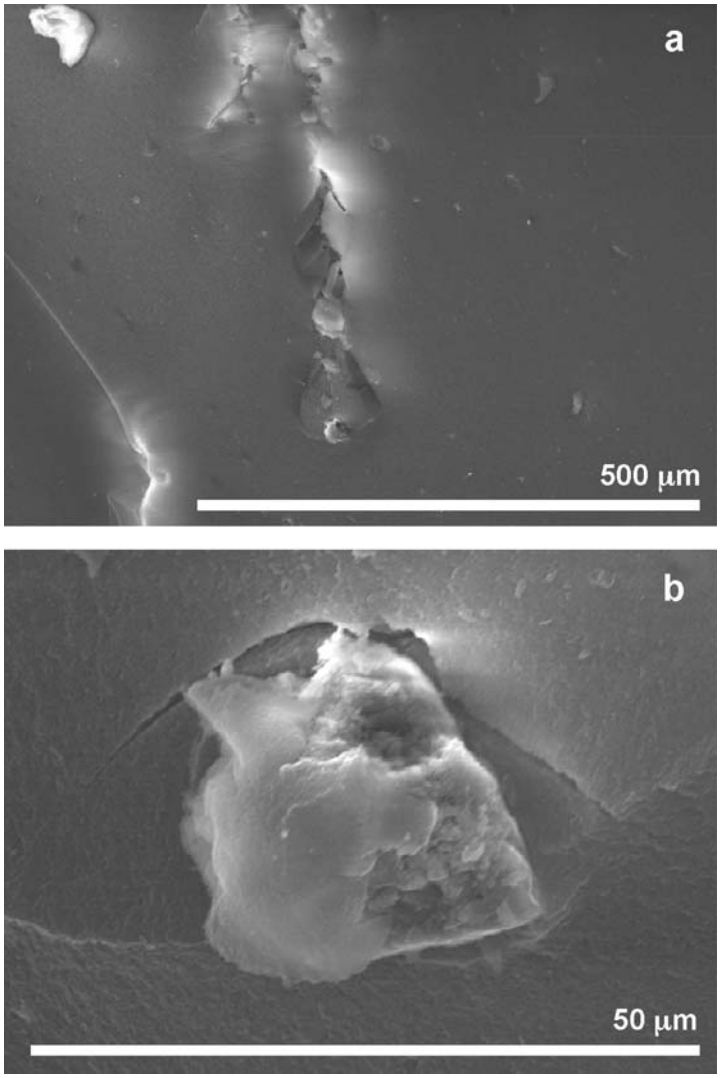

Figure 8

Secondary electron images of (*a*) an aerogel track and (*b*) a captured particle at the end of a track.

authors for example have found that the most effective and least damaging method for mounting millimeter-scale aerogel samples of complex shape for SEM is to lay the specimen on a clean aluminum stub and gently lay a strip of aluminized adhesive tape over an unimportant part of the surface, touching down each end to the underlying stub and thereby restraining movement of the caged aerogel. The sample can be easily removed later for analysis by other methods or for further preparation.

Small aerogel samples [especially the isolated keystones and nanokeystones of Westphal et al. (2004)] may be mounted, transported, and examined while securely held on silicon "micro pickle-forks" or even a hypodermic needle tip. Providing

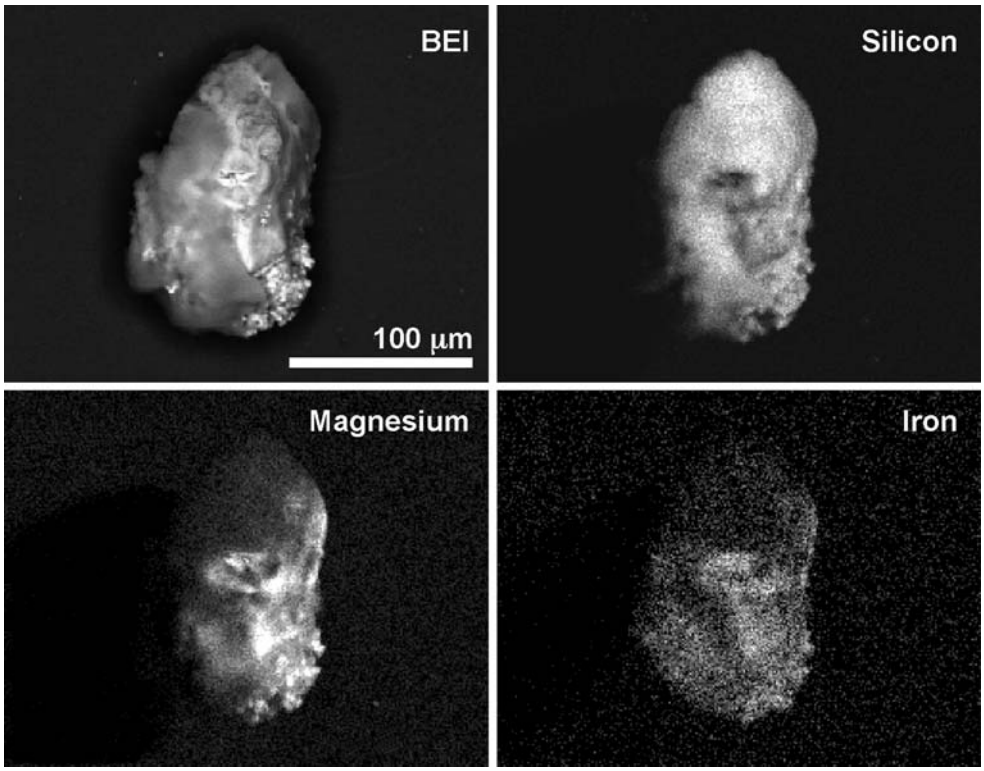

Figure 9

Backscattered electron image (*top left*) and X-ray maps of particle captured in aerogel, showing distribution of elements.

BEI: backscattered electron image

vibration of the mount is properly damped, such samples can successfully survive the buffeting of air or surface transport between laboratories without damage or loss. Although SEI of uncoated aerogel specimens at high vacuum is difficult, backscattered electron imagery (BEI) is usually successful (**Figures 9** and **10**) in revealing surface topographic features, textures, and some compositional contrast between the aerogel substrate and captured material. BEI of aerogel split open along track lengths reveals impact tracks with brecciated aerogel along the walls.

The problems of sample charging have now been largely sidestepped by the advent of low-vacuum or variable-pressure SEMs, which we have found to be well suited to examination of aerogel, in both backscattered electron and secondary electron modes. The beam scattering and reduction in signal level associated with use of a chamber pressure of 20 Pa is acceptable for the SEI of micrometer-scale surface features, although not rivaling the quality of SEIs generated by FIB microscopes. Beam dispersion caused by the presence of low-pressure gas, together with interaction volume effects described below, may also cause substantial degradation to the spatial resolution of X-ray microanalysis.

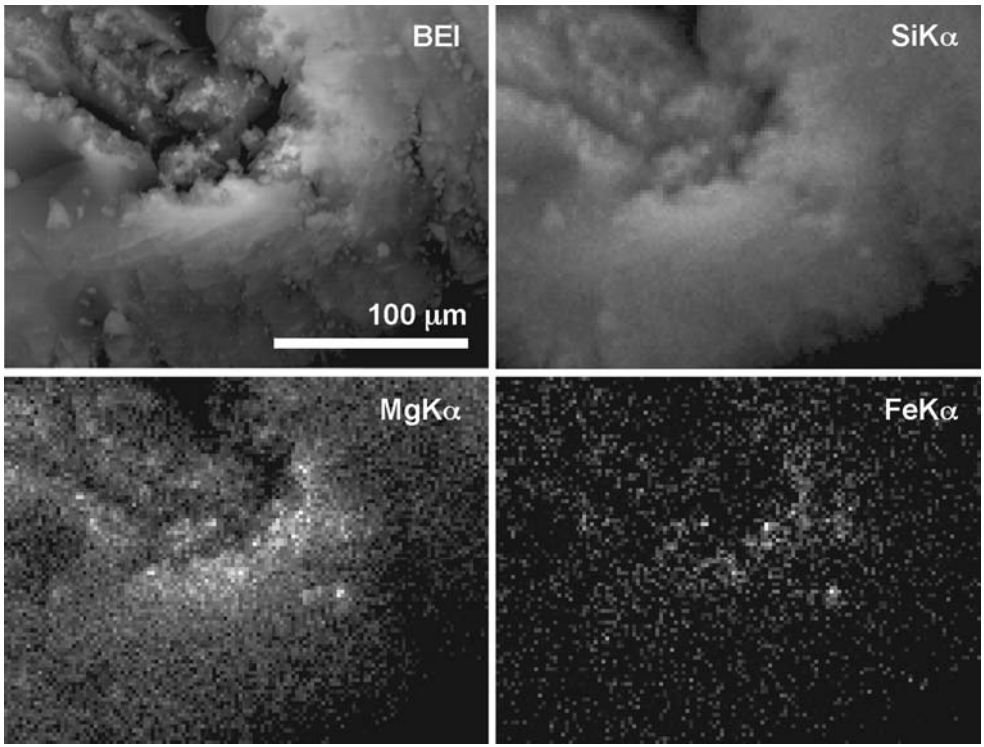

Figure 10

Backscattered electron image and X-ray maps of the same region as analyzed in **Figure 11** showing distribution of the captured residues. The track enters from the top left and stops approximately in the center of each image.

Optical microscopy and SEM on exposed surfaces of aerogel samples returned from orbit [e.g., ODC (Hörz et al. 2000)] or impacted in the laboratory (by light gas gun shots) usually shows fine-scale fracturing of aerogel along the impact track and creation of a thin envelope adhering to the surface of any surviving impactor grains. The envelope is not usually sufficiently thick as to prevent escape of high-energy electrons, backscattered from the underlying grain, but effectively prevents examination of the underlying grain surface by the high-resolution, low-energy electron beam of field emission microscopes. The choice of a relatively high beam accelerating voltage is thus critical to success in location of particle residue owing to the necessity of collecting data from below the immediate surface of the sample. However, despite the major difference in density between the aerogel (e.g., 15 kg m^{-3} to 100 kg m^{-3}) and most trapped particle compositions (e.g., pyroxene of density 2800 kg m^{-3}), there may be surprisingly little apparent contrast seen within electron images of an impact track. Although the depth of beam penetration is strongly influenced by the substrate density, this is counterbalanced by the enhanced proportion of electrons able to escape from greater depth. As a consequence, the backscattered electron coefficient of

EDS: energy dispersive X-ray spectra

PIXE: proton-induced X-ray emission

compounds is relatively insensitive to sample density, although strongly dependent on the atomic number of the component elements. Compositional information is thus available in the electron signal derived from tens of micrometers below the surface, rather than from the very shallow zone typical of most materials. However, the inherent compositional contrast between aerogel and common meteoritic silicate minerals is relatively small. The subtle patterns of compositional contrast may be overwhelmed easily by effects of complex variation in electron escape from the jagged topography of the fractured aerogel, generating a confusing range of image tones. Nevertheless, the deep beam penetration does stimulate characteristic X-ray emission from many micrometers below the surface, and this may be used to locate and analyze trapped particles. Energy dispersive X-ray spectra (EDS) collected from grains in the surface of impact tracks may give diagnostic compositional information, and X-ray maps of the track terminus are often successful in locating concentrations of fine fragments (**Figures 10** and **11**).

There may be substantial problems of X-ray absorption during transit from depth (Flynn et al. 1996, 2000; Westphal et al. 2003). This may result in low efficiencies of signal collection for lower energy X-ray lines (1500 eV and less), resulting in the potential for misidentification of the analyzed particle if peak area ratios are used as a diagnostic indicator. A similar problem is encountered in all techniques that rely on escape of X-rays from an embedded particle, e.g., proton-induced X-ray emission (PIXE) and synchrotron X-ray fluorescence, although the very high flux of these

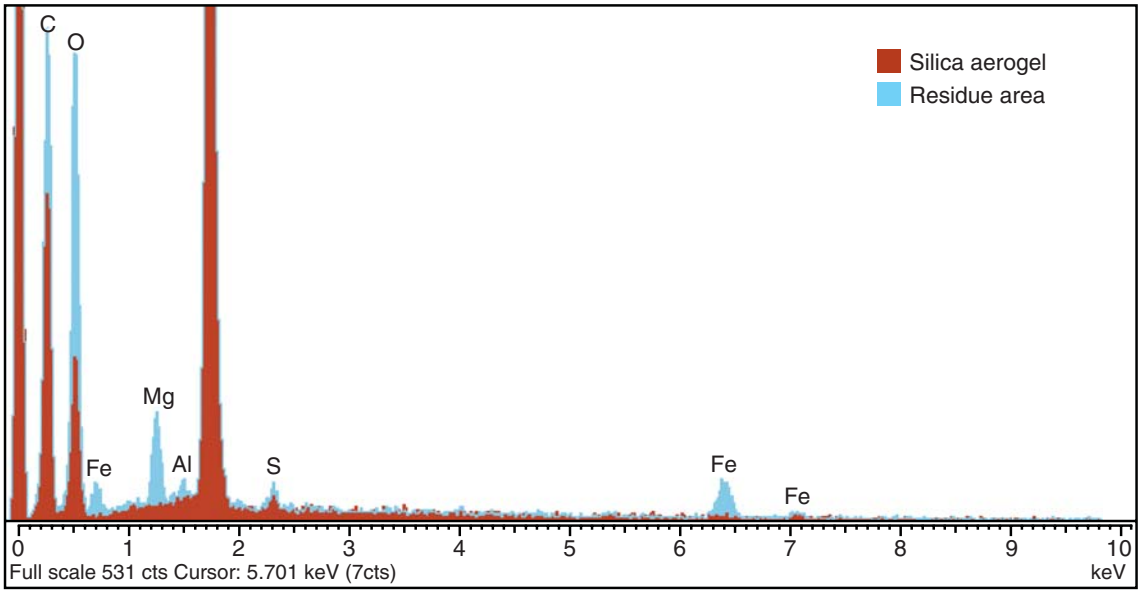

Figure 11

X-ray spectra taken from an area at the end of a track in aerogel. Blue is from the area of interest, overlapped on red (the background from a similar volume of aerogel away from the track). Carbon, oxygen, iron, magnesium, and aluminum are present in particle residue.

latter techniques may considerably reduce effective lower detection limits. The effect of absorption along the path length may also be monitored by examination of the brehmstrahlung X-ray continuum shape for evidence of low-energy X-ray suppression. Fortunately, materials with a relatively high backscattered electron coefficient and high-energy characteristic X-ray emission lines (such as transition metals, their oxides, and sulfides) may be recognized well below the surface. The low X-ray count rate may require long spectrum and map acquisition times, and the use of high electron beam currents for an acceptable spectrum to be obtained. This, in turn, may lead to problems with instrument artifacts, such as sum peaks, that must be carefully identified lest they give a misleading identification of small characteristic emission line peaks.

STIM: scanning transmission ion microscopy

PESA: proton elastic scattering analysis

PBS: proton backscattering

Particle mass may be ablated during creation of the impact track (see above), with deposition of submicrometer-scale residue along and within the track walls. Such diffuse material may be detected in long-duration X-ray emission maps of open track surfaces. However, prolonged irradiation of aerogel areas with a high-energy beam at high beam current (e.g., 40 keV and 2nA) may result in discoloration, possibly as a function of thermal maturation of organic matter indigenous to the aerogel, and also owing to deposition of surface contamination from the vacuum system if imaged in a microscope employing an oil diffusion pump. In experiments by the authors, a small area (500 × 380 micrometers) of low-density aerogel (19 kg m^{-3}) was irradiated in a LEO 1455VP SEM with turbo-molecular pumping for 18 h, beneath a scanning beam of 20keV energy and 1nA current in high vacuum. The irradiated area was then examined under an optical microscope, which revealed a rectangular area of brown discoloration. Another aerogel sample irradiated at high vacuum in a JEOL 5900LV SEM with oil diffusion pump vacuum system, again at 1nA and 20keV, gave a similar result. We conclude that the alteration is probably a function of thermal maturation of organic matter indigenous to the aerogel, as it is found even where there is unlikely to be deposition of surface contamination from the vacuum system. A novel SEM method to locate particles at depth within aerogel samples without direct electron beam irradiation has been reported by Graham et al. (2005), employing a point X-ray source stimulated by the electron beam, projection through the aerogel block, and X-ray capture on a large area charge-coupled device detector. This may be used to generate three-dimensional images similar to conventional X-ray tomography.

More detailed analysis methods can also be readily applied to exposed samples. SEM and STEM have been demonstrated on particles captured in aerogel and then removed using the keystone approach described above (Westphal et al. 2004). More elaborate approaches are also available. For example, scanning transmission ion microscopy (STIM) can be applied to measure column densities in small samples. In this way, small particles can be found embedded in aerogel. This has been demonstrated for particles of size down to order 10 microns placed in aerogel samples (Graham et al. 2004b). It is not clear how a molten wrap of aerogel (which can be acquired during a hypervelocity capture) would affect such an analysis, but the method is promising and may be applicable at particle sizes down to 1 micron.

Analysis of samples via proton elastic scattering analysis (PESA) and proton backscattering (PBS) is also possible (Graham et al. 2004b). In PESA, the scattered protons transfer energy to the target atoms depending on their mass and so a

measurement of the energy loss of the scattered ions gives a measure of the mass of the target atom. Using a 3 MeV proton beam, Graham et al. (2004b) scanned an aerogel block with particles embedded in it by hand. The resulting distribution map for hydrogen indicated the location of particles of polystyrene and Orgueil meteorite in the aerogel. Further, when subtraction of the component of signal from the aerogel itself was made, quantifiable estimates of the hydrogen content of the captured particles was possible. By measuring the energy of backscattered protons in the same setup, it was possible to obtain estimates of other elemental components of the particles. Carbon, oxygen, silicon, and iron could all be identified and their presence in the particles quantified after subtraction of contributions from the aerogel itself. This method cannot identify the origin of the carbon as being organic or inorganic, but it can identify carbon-rich particles for further analysis.

As well as PESA and PBS, if a high-energy proton beam is used for materials characterization, then PIXE is possible on samples in aerogel. This is not well suited for identification of light elements ($Z < 11$), but works satisfactorily for elements such as oxygen, silicon, iron, tungsten, etc. Combining these techniques (STIM, PESA, PSA, and PIXE), Graham et al. (2004b) were able to account for over 95 weight% of the elemental total for a chondritic particle trapped in aerogel. However, with all these ion beam techniques, there is the risk of damage to the samples owing to the high beam currents required. Further, there is a risk the stoichiometry in a sample may be altered by the damage during analysis.

The damage to samples by ion beams can be turned to advantage. FIB microscopy uses a beam of ions (typically Ga) to ablate samples under controlled conditions. This can operate at the micron scale, removing coatings of aerogel and cutting trenches into the captured particles exposing the relatively undamaged interior. FIB microscopy typically incorporates STEM, electron diffraction techniques, and EDS to characterize the freshly exposed material. Although destructive, it is a powerful tool for mineralogical characterization of samples at micron scales.

CONCLUSIONS

Aerogel has now been used for almost two decades to capture particles at high speed. It has been extensively deployed in space, and suitable extraction and analysis techniques have been developed for the captured cosmic dust. The return of the Stardust cometary dust samples in 2006 will undoubtedly trigger a major burst of interest in capture of dust in aerogel. For most researchers, the aerogel will be of no interest, it is study of the dust that is the real scientific goal. Based on the work reviewed above, such researchers can have confidence that a sufficient understanding of aerogel and its use as a capture medium has been obtained. Analysis techniques (a range of which have been outlined here) are sufficiently developed and tested to permit the detailed study of captured dust. Aerogel capture cells can thus be considered to have reached maturity as a scientific method for the study of cosmic dust.

The dust extracted from aerogel contains unaltered samples of the original grains (if the original particle was sufficiently robust). These are, in general, far superior to the residues (found in impact craters) currently used to analyze cosmic dust. The

sizes and volumes will be in nanograms, but for current analysis techniques this is not an issue. Although some analysis can be applied in situ, more detailed analysis requires that the particle either be exposed on a cut aerogel surface or completely extracted. This can then permit a precise mineral composition involving interelement stoichiometric ratios. For analysis of volatile and organic components, there may be difficulties related to heating and contamination during the capture process that limit the precision of any subsequent analysis. Nevertheless, some organic analysis is possible, as described above.

One difficulty with capture in aerogel lies in the treatment of submicron grains. It is not clear how these can be found optically (although the larger tracks may be visible at the micron scale, the captured particle will not be). Nor is it clear how these could be found by any other spectroscopic analysis technique. This may well set a lower limit to the size of particles that can be studied after capture in aerogel.

Overall, aerogel offers a readily usable medium for capturing cosmic dust in space. The next decade will see more use of it and a growing volume of scientific results based on captured cosmic dust.

SUMMARY POINTS

1. Aerogel can be used to capture particles at impact speeds up to 10+ km s^{-1}.
2. The captured particles are not fully intact and usually have undergone loss of mass during capture.
3. The captured particles in laboratory studies all retain unaltered domains, which yield their original structure and composition.
4. Analysis of the captured particles can be done either in situ or after extraction.
5. Aerogel has already been successfully deployed in space in LEO and retrieved with extraterrestrial material in it.
6. The NASA Stardust mission will return aerogel samples to Earth in January 2006, with dust captured during a fly-by of comet P/Wild-2.
7. Aerogel capture cells can now be considered a mature technology, providing understandable results for studies of cosmic dust.

FUTURE DIRECTIONS

1. A detailed model of capture in aerogel still needs to be properly developed.
2. How to find and analyze submicron grains captured in aerogel remains to be demonstrated.
3. For general use, dust collectors with aerogel integrated into an active electronic detector or other methods (for timing of impacts and impact speed measurements) still need to be demonstrated.

ACKNOWLEDGMENTS

Giles Graham's recent work was performed in part under the auspices of the U.S. Department of Energy by the Lawrence Livermore National Laboratory under Contract No. W-7405-ENG-48.

LITERATURE CITED

Adachi I, Sumiyoshi T, Hayashi K, Iida N, Enomto E, et al. 1995. Study of a threshold Cherenkov counter based on silica aerogels with low refractive indices. *Nucl. Instr. Methods* A355:390–98

Anderson WW, Ahrens TJ. 1994 Physics of interplanetary dust capture via impact into organic polymer foams. *J. Geophys. Res.* 99(E1):2063–71

Auer S. 1998. Impact ionization from silica aerogel. *Int. J. Impact Eng.* 21:89–95

Auer S. 2001. Instrumentation. See Grün et al. 2001, pp. 385–444. Berlin: Springer-Verlag. 804 pp.

Barrett RA, Zolensky ME, Hörz F, Lindstrom DJ, Gibson EK. 1992. Suitability of silica aerogel as a capture medium for interplanetary dust. *Proc. Lunar Planet. Sci. Conf.* 22:203–12

Bradley JP, Brownlee DE, Veblen DR. 1983. Pyroxene whiskers and platelets in interplanetary dust—evidence of vapour phase growth. *Nature* 301:473–77

Brownlee DE. 1985. Cosmic dust: collection and research. *Annu. Rev. Earth Planet. Sci.* 13:147–73

Brownlee DE, Horz F, Hrubsch L, McDonnell JAM. 1994. Eureka!! Aerogel capture of micrometeoroids in space. *Lunar Planet. Sci. Conf. Abstr.* XXV:183–84

Brownlee DE, Tsou P, Anderson JD, Hanner MS, Newburn RL, et al. 2003. Stardust: comet and interstellar dust sample return mission. *J. Geophys. Res.* 108(E10):8111

Bunch TE, Schultz P, Cassen P, Brownlee D, Podolak M, et al. 1991. Are some chondrule rims formed by impact processes? Observations and experiment. *Icarus* 91:76–92

Burchell MJ, Cole MJ, McDonnell JAM, Zarnecki JC. 1999a. Hypervelocity impact studies using the 2 MV Van de Graaff dust accelerator and two stage light gas gun of the University of Kent at Canterbury. *Meas. Sci. Technol.* 10:41–50

Burchell MJ, Creighton JA, Cole MJ, Mann J, Kearsley AT. 2001. Capture of particles in hypervelocity impacts in aerogel. *Meteorit. Planet. Sci.* 36:209–21

Burchell MJ, Creighton JA, Kearlsey AT. 2004. Identification of organic particles via Raman techniques after capture in hypervelocity impacts on aerogel. *J. Raman Spectr.* 35:249–53

Burchell MJ, Mann J, Creighton JA, Kearsley AT, Franchi A. 2006. Identification of minerals and meteoritic materials via Raman techniques after capture in hypervelocity impacts on aerogel. *Meteorit. Planet. Sci.* In press

Burchell MJ, Thomson R. 1996. Intact hypervelocity particle capture in aerogel in the laboratory. *Shock Compression of Condensed Matter-1997*, Conf Proc. 429, pp. 1155–58. New York: AIP Press

Burchell MJ, Thomson R, Yano H. 1999b. Capture of hypervelocity particles in aerogel: in ground laboratory and low earth orbit. *Planet. Space Sci.* 47:189–204

Domínguez G, Westphal AJ, Phillips MLF, Jones SM. 2003. A fluorescent aerogel for capture and identification of interplanetary and interstellar dust. *Astrophys. J.* 592:631–35

Domínguez G, Westphal AJ, Jones SM, Phillips MJF. 2004. Energy loss and impact cratering in aerogels: theory and experiment. *Icarus* 172:613–24

Flynn GJ, Horz F, Bajt S, Sutton SR. 1996. In-situ chemical analysis of extraterrestrial material captured in aerogel. *Lunar Planet. Sci. Conf. Abstr.* XXVII:369–70

Flynn GJ, Sutton SR, Hörz F. 2000. Synchrotron X-ray microprobe in-situ analysis of extraterrestrial particles collected in aerogel on the Mir Space Station. *Lunar Planet. Sci. Conf. Abstr.* XXXI:1457

Foster N. 2006. *Synthesis of silica aerogel and its application as a hypervelocity dust capture cell*. MSc. thesis, Univ. of Kent.

Gibiat V, Lefeuvre O, Woignier T, Pelous J, Phalippou J. 1995. Acoustic properties and potential applications of silica aerogels. *J. Non-Crystal. Solids* 186:244–55

Gibson JE, Pillinger CT, Gibson EK. 1991. Carbon content of silica aerogel: a material proposed as a medium for collection of cosmic grains. *Lunar Planet. Sci. Conf. Abstr.* XXII:441–42

Graham GA, Kearsley AT, Wright IP, Burchell MJ, Taylor EA. 2003. Observations on hypervelocity impact damage sustained by multi-layered insulation foils exposed in low earth orbit and simulated in the laboratory. *Int. J. Impact Eng.* 29:307–16

Graham GA, Kearsley AT, Butterworth AL, Bland PA, Burchell MJ, et al. 2004a. Extraction and microanalysis of cosmic dust collected during sample return missions: laboratory simulations. *Adv. Space Res.* 34:2292–98

Graham GA, Grant PG, Chater RJ, Westphal AJ, Kearsley AT, et al. 2004b. Investigation of ion beam techniques for the analysis and exposure of particles encapsulated by silica aerogel: applicability for Stardust. *Meteorit. Planet. Sci.* 39(9):1461–73

Graham GA, Sheffield-Parker J, Bradley JP, Kearsley AT, Dai ZR, et al. 2005. Electron beam analysis of micrometeoroids captured in aerogel as Stardust analogues. *Lunar Planet. Sci. Conf. Abstr.* XXXVI:2078

Graps AL, Grün E, Svedhen H, Krüger H, Horányi H, et al. 2000. Io as a source of the Jovian dust streams. *Nature* 405:48–50

Grover R, Ree F, Holmes N. 1992. Equation of state from SiO_2 Aerogel Hugoniot Data, *Shock Compression of Condensed Matter 1991*, Conf. Proc. 370, pp. 95–98. New York: AIP Press

Grün E, Gustafson BÅS, Dermott SF, Fechtig H, eds. 2001. *Interplanetary Dust*. Berlin: Springer-Verlag. 804 pp.

Grün E, Zook HA, Baghul M, Balogh A, Bame SJ, et al. 1993 Discovery of Jovian dust streams and interstellar grains by the Ulysses Spacecraft. *Nature* 362:428–30

Hartmetz CP, Gibson EK, Blanford GE. 1990a. In-situ extraction and analysis of volatiles and simple molecules in interplanetary dust particles, contaminants, and silica aerogel. *Proc. 20th Lunar Planet. Sci. Conf.*, pp. 343–55

Hartmetz CP, Gibson EK, Lauer HV. 1990b. A study of aerogel's suitability as an IDP collection substrate: potential solutions to volatile contamination problems. *Lunar Planet. Sci. Conf. Abstr.* XXI:463–64

Holmes NC, See EF. 1992. Shock compression of low density microcellular materials, *Shock Compression of Condensed Matter 1991*, Conf. Proc. 370, pp. 91–94, New York: AIP Press

Hörz F, Cintala MJ, Zolensky ME. 1992. Hypervelocity penetration tracks in very low density, porous targets. See McDonnell 1992, pp. 19–23

Hörz F, Cintala MJ, Zolensky ME, Bernhard RB, Davidson WE, et al. 1998. Capture of hypervelocity particles with low density aerogel. *NASA TM-98-201792*

Hörz F, Zolensky ME, Bernhard RP, See TH, Warren JL. 2000. Impact features and projectile residues in aerogel exposed on Mir. *Icarus* 147:559–79

Hrubesh LW, Poco JF. 1990. *Development* of low density silica aerogel. UCRL Preprint CR105858-SUM, Lawrence Livermore Natl. Lab., Berkeley, CA

Hrubesh LW. 1998. Aerogel Applications. *J. Non-Crystal. Solids* 225:335–42

Huang HP, Gilmour I, Pillinger CT. 1993. Removal of carbonaceous contaminants from silica aerogel. *Lunar Planet. Sci. Conf. Abstr.* XXIV:679–80

Ishibashi T, Fujiwara A, Fujii N. 1990. Penetration of hypervelocity projectiles into foamed polystyrene. *Jap. J. Appl. Phys* 29:2543–48

Ishii HA, Graham GA, Kearsley AT, Grant PG, Snead CJ, Bradley JP. 2005. Ultrasonic micro-blades for the rapid extraction of impact tracks from aerogel. *Lunar Planet. Sci. Conf. Abstr.* XXXVI:1387

Kadono T. 1999. Hypervelocity Impacts onto low density material and cometary outburst. *Planet. Space Sci.* 47:305–18

Kearsley AT, Burchell MJ, Graham GA, Cole MJ, Wallis D. 2005. Interpreting micrometeoroid residues on metallic spacecraft surfaces: clues from low Earth orbit, the laboratory and to come from Stardust? *Lunar Planet. Sci. Conf. Abstr.* XXXVI:1670

Kempf S, Srama R, Postberg F, Burton M, Green SF, et al. 2005. Composition of Saturn stream particles. *Science* 307:1274–76

Kissel J, Glasmachers A, Grün E, Henkel H, Höfner H, et al. 2003. Cometary and interstellar dust analyzer for comet Wild 2. *J. Geophys. Res.* 108(E10):8114

Kissel J, Krueger FR, Silén J, Clark BC. 2004. The cometary and interstellar dust analyzer at comet 81P/Wild2. *Science* 304:1774–76

Kistler SS. 1931. Coherent expanded aerogels and jellies. *Nature* 127:741

Kitazawa Y, Fujiwara A, Kadono T, Imagawa K, Okada Y, Uematsu K. 1999. Hypervelocity impact experiments on aerogel dust collector. *J. Geophys. Res.* 104(E9):22035–52

Kitazawa Y, Noguchi T, Neish MJ, Inoue T, Ishizawa J, et al. 2004. First year mission results of passive measurement experiment of dust particles on ISS (MPAC). Presented at *Int. Symp. Space Technol. Sci., 24th*, ISTC 2004-r-6, Tokyo

Maag C, Kelly Linder W. 1992. Results of space shuttle intact capture experiments. See McDonnell 1992, pp. 186–90

McDonnell JAM. 1992. *Hypervelocity Impacts in Space*. Caterbury, UK: Univ. of Kent. 288 pp.

McDonnell JAM, Carey WC, Dixon DG. 1984. Cosmic dust capture collection by the capture cell technique on the space shuttle. *Nature* 309:237–40

McDonnell JAM, Burchell MJ, Green SF, Leese M, Wallis D, et al. 2000. APSIS—aerogel position-sensitive impact sensor: capabilities for in-situ collection and sample return. *Adv. Space Res.* 25(2):315–22

Okudaira K, Noguchi T, Nakamura T, Sugita S, Sekine Y, Yano H. 2004. Evaluation of mineralogical alteration of micrometeoroid analog materials captured in aerogel. *Adv. Space Res.* 34:2299–304

Okudaira K, Yano H, Noguchi T, Nakamura T, Burchell MJ, Cole MJ. 2005. Are they really intact? Evaluation of captured micrometeoroid analogs by aerogel at the flyby speed of Stardust. *Lunar Planet. Sci. Conf. Abstr.* XXXVI:1832

Nishioka K, Bunch T, Fonda M, Ryder JT, Wittenauer J. 1996. Aerogel for IDP capture: lessons learnt. *Lunar Planet. Sci. Conf. Abstr.* XXVII:963–64

Poelz G, Reithmuller R. 1982. Preparation of silica aerogel for Cherenkov counters. *Nucl. Instr. Methods* 195:491–503

Shrine NRG, McDonnell JAM, Burchell MJ, Gardner DJ, Jolly HS, et al. 1997. EuroMir '95: first results from the dustwatch-P detectors of the European Space Exposure Facility. *Adv. Space Res.* 20(8):1481–84

Tedeschi WJ, Remo JL, Schulze JF, Young RP. 1995. Experimental hypervelocity impact effects on simulated planetesimal materials. *Int. J. Impact Eng.* 17:837–48

Tillotson TM, Hrubesh LW. 1992. Transparent ultra-low density silica aerogels prepared by a two-step sol gel process. *J. Non-Crystal. Solids* 145:44–50

Tsou P. 1990. Intact capture of hypervelocity projectiles. *Int. J. Impact Eng.* 10:615–27

Tsou P. 1995. Silica aerogel captures cosmic dust intact. *J. Non-Crystal. Solids* 186:415–27

Tsou P, Aubert J, Brownlee D, Hrubesh L, Williams J, Albee A. 1989. Effectiveness of intact capture media. *Lunar Planet. Sci. Conf. Abstr.* XX:1132–33

Tsou P, Bradley JP, Brownlee DE, Fechtig H, Hrubesh FL, et al. 1990. Intact capture of cosmic dust analogs in aerogel. *Lunar Planet. Sci. Conf. Abstr.* XXI:1264–65

Tsou P, Brownlee DE, Albee AL. 1993. Intact capture of hypervelocity particles on shuttle. *Lunar Planet. Sci. Conf. Abstr.* XXIV:1443–44

Tsou P, Brownlee DE, Laurance MR, Hrubesh L, Albee AL. 1988. Intact capture of hypervelocity micrometeoroid analogs. *Lunar Planet. Sci. Conf. Abstr.* XIX:1205–6

Tsou P, Brownlee DE, Sandford SA, Zolensky ME. 2003. Wild-2 and Intersteller sample collection and Earth return. *J. Geophys. Res.* 108(E10):8113

Tsou P, Brownlee DE, Williams JE, Albee AL. 1991. Effects of media mesostructure on intact capture. *Lunar Planet. Sci. Conf. Abstr.* XXII:1419–20

Tuzzolino AJ, Economou TE, McKibben RB, Simpson JA, McDonnell JAM, et al. 2003. Dust flux monitor instrument for the Stardust mission to comet Wild 2. *J. Geophys. Res.* 108(E10):8115

Tuzzolino AJ, Economou TE, Clark BC, Tsou P, Brownlee DE, et al. 2004. Dust measurements in the coma of comet 81P/Wild 2 by the dust flux monitor instrument. *Science* 304:1776–80

Werle V, Fechtig H, Schneider E. 1981. Impact accretion experiments. *Proc. Lunar Planet. Sci. Conf.* 12B:1641–47

Westphal AJ, Snead C, Borg J, Quirico E, Raynal P-I, et al. 2002. Small hypervelocity particles captured in aerogel collectors: Location, extraction, handling and storage. *Meteorit. Planet. Sci.* 37:855–65

Westphal AJ, Snead C, Butterworth A, Graham GA, Bradley JP, et al. 2004. Aerogel keystones: extraction of complete hypervelocity impact events from aerogel collectors. *Meteorit. Planet. Sci.* 39:1375–86

Westphal AJ, Snead C, Dománguez G. 2003. An extraction and curation technique for particles captured in aerogel. *Lunar Planet. Sci. Conf. Abstr*. XXXIV:1826

Wright IP, Huang HP, Pillinger CT. 1994. Attempts to produce carbon-free silica aerogel for micrometeoroid capture cells. *Lunar Planet. Sci. Conf. Abstr.* XXV:1515–16

Yano H, Arakawa M, Michikami T, Fujiwari A. 1999. Sub-millimeter sized ice grain impacts on aerogels; implications to a cometary dust sample return mission. *Lunar Planet. Sci. Conf. Abstr.* XXX:1961

Zolensky ME, Barrett RA, Horz F, Cardenas F, Davidson W, et al. 1989. The utility of silica aerogel as a cosmic dust capture medium on the space station. *Lunar Planet. Sci. Conf. Abstr.* XX:1251–51

Zolensky ME, Barrett RA, Hrubesh L, Horz F, Lindstrom D. 1990. Cosmic dust capture simulation experiments using silica aerogels. *Lunar Planet. Sci. Conf. Abstr.* XXI:1381–82

Zolensky M, Pieters C, Clark B, Papike JJ. 2000. Small is beautiful, the analysis of nano-gram sized astromaterials. *Meteorit. Planet. Sci.* 35:9–29

Zolensky M, Sandford S, Hörz F, Brownlee D, Tsou P, Clark B. 2004. Preliminary sample analysis plan for the cometary and interstellar samples being returned by the Stardust spacecraft. *Lunar Planet. Sci. Conf. Abstr.* XXXV:1367

RELATED RESOURCE

Brownlee DE. 1985. Cosmic dust: collection and research. *Annu. Rev. Earth Planet. Sci*. 13:147–73

Annual Review of Earth and Planetary Sciences

Volume 34, 2006

Contents